NRC Research Press

ARTICLE

Photoswitchable organoplatinum complexes containing an azobenzene derivative of 3,6-di(2-pyridyl)pyridazine

Mohamed E. Moustafa, Paul D. Boyle, and Richard J. Puddephatt

Abstract: The new, unsymmetrical azobenzene-tagged ligand 4-(4-azobenzene)-3,6-di(2-pyridyl)pyridazine, adpp, forms complexes with platinum(II) and platinum(IV), which exist as a mixture of geometrical isomers. The complexes are characterized primarily by their NMR spectra, while the structures of the ligand and its complexes [$PtMe_2$(adpp)], [$PtBrMe_2(CH_2C_6H_4$-4-*t*-Bu)(adpp)], and [$PtBrMe_2(CH_2C_6H_3$-3,5-*t*-Bu_2)(adpp)] have been structurally characterized. In solution, the compounds undergo easy photochemical *trans–cis* switching of the azobenzene group, with subsequent slow thermal isomerization back to the more stable *trans*-azobenzene isomer.

Key words: platinum, azobenzene, photochemistry, organometallic.

Résumé : Le nouveau ligand marqué par l'azobenzène, la 4-(4-azobenzene)-3,6-di(2-pyridyl)pyridazine, ou adpp, forme des complexes avec le platine(II) et le platine(IV), présents sous forme d'un mélange d'isomères géométriques. Les complexes sont principalement caractérisés à l'aide de leur spectre RMN et le ligand et ses complexes, [$PtMe_2$(adpp)], [$PtBrMe_2(CH_2C_6H_4$-4-*t*-Bu)(adpp)] et [$PtBrMe_2(CH_2C_6H_3$-3,5-*t*-Bu_2)(adpp)] par leur structure chimique. En solution, les composés subissent facilement une transposition photochimique *trans–cis* du groupe azobenzène, qui redevient, par isomérisation thermique lente, l'isomère *trans*-azobenzène, plus stable. [Traduit par la Rédaction]

Mots-clés : platine, azobenzéne, photochimie, organométallique.

Introduction

There is continuing interest in the use of azobenzene derivatives in artificial photochromic systems because the azobenzene unit can be switched reversibly between *trans* and *cis* isomers, which have different electronic and structural properties.[1,2] Typically, the more stable *trans* isomer can be converted to the *cis* isomer by irradiation into its $\pi-\pi^*$ band centred at about 340 nm, while the *cis* isomer can be converted back to the *trans* isomer either by mild heating or by irradiation into its $\pi-\pi^*$ band centred at about 450 nm (Scheme 1). The isomerization can be monitored easily by taking advantage of the major differences in the UV-visible or ^{1}H NMR spectra of the isomers, while the high stability of azobenzene allows many switching cycles to be achieved without significant decomposition.[1–4]

There are still rather few photoswitchable organometallic complexes[5–9] and the first photoswitchable organoplatinum complexes were reported only recently.[10,11] Selected examples are shown in Scheme 2. The azobenzene group has been incorporated into a pyridyl-imine ligand in the platinum(II) complex ***A*** and into an alkylplatinum group in the platinum(IV) complex ***B***.

In both ***A*** and ***B*** (Scheme 2), the azobenzene is only one atom (nitrogen atom in ***A***, carbon atom in ***B***) removed from the platinum centre, but photoswitching was more efficient for ***B***, in which the azobenzene group is separated from platinum by a saturated carbon centre, than for ***A***, in which conjugation of the π-systems of the azobenzene and platinum-imine groups is possible.[10,11] The present work describes the synthesis and photochemistry of an azobenzene-tagged 3,6-di(2-pyridyl)pyridazine ligand and its corresponding complexes with platinum(II) and platinum(IV), in which the azobenzene group is further removed from the platinum centre but in which π-conjugation is possible. The ligand 3,6-di(2-pyridyl)pyridazine and its derivatives are known to form stable complexes with transition metals, including copper,[12] silver,[13,14] ruthenium,[15,16] and platinum.[17–19] Pyridazines have also been utilized in the framework for the synthesis of metal organic frameworks.[20,21]

Results and discussion

The synthesis of the new azobenzene-tagged ligand 4-(4-azobenzene)-3,6-di(2-pyridyl)pyridazine, adpp, is shown in Scheme 3. The first steps lead to the synthesis of the alkyne 4-ethynylazobenzene, EAB, according to the published procedure,[22,23] while the second step involves the reaction of 3,6-di(2-pyridyl)-1,2,4,5-tetrazine with the alkyne with displacement of dinitrogen.[24] This final reaction is an inverse electron demand Diels–Alder reaction and has been used to prepare several other derivatives of 3,6-di(2-pyridyl)pyridazine.[24] As this reaction occurs, the purple colour of the tetrazine is replaced by the orange colour of adpp.

The structure of the ligand adpp is shown in Fig. 1 and confirms the expected *trans* stereochemistry of the azobenzene group. Notably, the ligand exhibits a conformation in which the neighbouring pyridine and pyridazine nitrogen atoms mutually *anti*, which is probably favoured by weak N··H hydrogen bonding interactions. The two pyridyl rings are twisted out of the plane of the pyridazine ring by 11° and 43° for the N(1) and N(4) rings, respectively, while the azobenzene C_6H_4 group is twisted out of the plane of the pyridazine ring by 43°. The greater twists for the N(4)

Received 9 January 2014. Accepted 5 February 2014.

M.E. Moustafa. Department of Chemistry, University of Western Ontario, London, ON N6A 5B7, Canada; Department of Chemistry, Faculty of Education, Suez Canal University, Arish, Egypt.
P.D. Boyle and R.J. Puddephatt. Department of Chemistry, University of Western Ontario, London, ON N6A 5B7, Canada.
Corresponding author: Richard J. Puddephatt (e-mail: pudd@uwo.ca).

This article is part of a Special Issue dedicated to Professor Barry Lever in recognition of his contributions to inorganic chemistry across Canada and beyond.

Scheme 1. Photoisomerization of azobenzene derivatives.

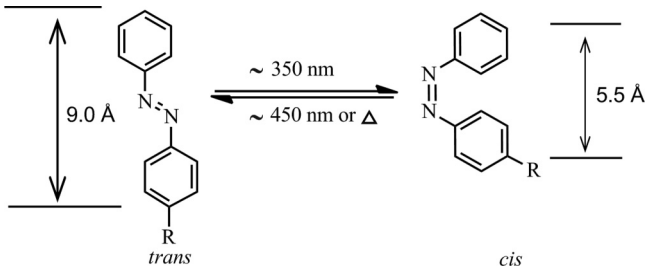

Scheme 2. Photoswitchable organoplatinum complexes (NN = 2,2′-bipyridine).

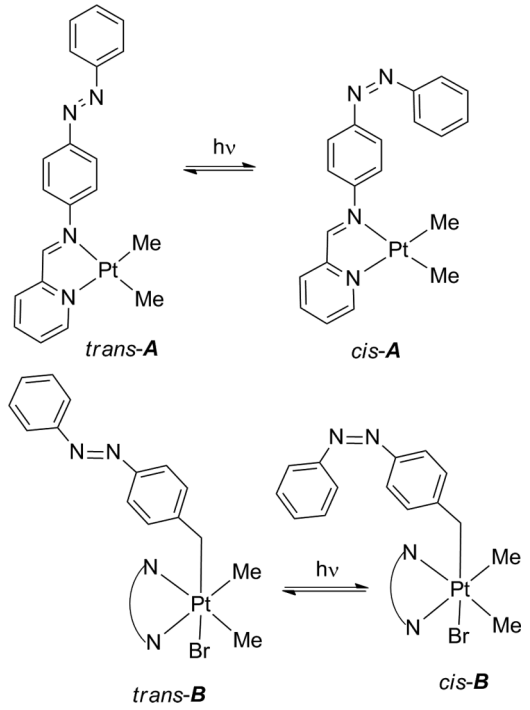

pyridyl ring and the C_6H_4 group are clearly to relieve steric congestion between these groups, but it occurs at the expense of π-conjugation and hydrogen bonding (compare N(3)··H(11) 2.65 Å, N(2)··H(4) 2.52 Å, and N(1)··H(7) 2.45 Å). The azobenzene atoms are close to being coplanar (twist between the two aryl groups is 7°).

The complex [$PtMe_2$(adpp)], **1**, was readily prepared by the reaction of the ligand adpp with the precursor [$Pt_2Me_4(\mu\text{-}SMe_2)_2$] in acetone,[25] with displacement of the dimethyl sulfide ligands (Scheme 4), and was isolated as a red solid. The ^{1}H NMR spectrum of complex **1** showed that it was formed as a mixture of isomers **1a** and **1b** in about an 85:15 ratio as determined by integration of the methylplatinum resonances (Fig. 2). Complex **1a** gave two methylplatinum resonances (δ 1.41 and 1.65, each with coupling constant ^2JPtH = 88 Hz), and a doublet resonance for the *ortho* hydrogen atom of the coordinated pyridine ring was observed at δ 9.40, with coupling constant ^3JPtH = 23 Hz, demonstrating chelation of platinum(II) by the ligand adpp. Isomer **1b** gave similar parameters (δ(MePt)1.40, ^2JPtH = 87 Hz; 1.62, ^2JPtH = 87 Hz; δ (H^6) 8.32, ^3JPtH = 23 Hz).

It was not possible to separate the isomers of complex **1**, but single crystals of the major isomer **1a** were obtained, as the chloroform solvate, and its structure is shown in Figs. 3 and 4. It shows that the 2-pyridyl group closer to the azobenzene coordinates to platinum in forming the chelate complex. The reason for this selectivity is not obvious, since chelation requires the N(1) pyridyl group to be roughly coplanar with the pyridazine group (twist angle is 11° compared to 43° in the free ligand adpp) and this increases steric effects with the azobenzene group when compared to the free ligand adpp. The structure of **1a** does, however, allow CH··N hydrogen bonding of the free 2-pyridyl group to be retained (N(3)··H(13) 2.52 Å, N(4)··H(10) 2.49 Å; twist angle of the N(4) pyridyl group is 14° compared to 11° in free adpp). The chloroform solvate molecule in **1a** is hydrogen bonded to the electron-rich dimethylplatinum(II) centre, with Pt(1)··H(1X) 2.65 Å, in the range found for similar interactions.[26–28] The flat structure of the di-2-pyridyl-pyridazine unit in **1a** allows π-stacking between pairs of molecules, as shown in Fig. 4. The isomers **1a** and **1b** do not easily interconvert at room temperature.

The reaction of the ligand adpp with *trans*-[PtCl(Me)(SMe_2)$_2$][11] in acetone afforded the complex [PtClMe(adpp)], **2**, as depicted in Scheme 5. The ^{1}H NMR spectrum of **2** showed that it was formed as a mixture of two isomers, with relative abundance of 65:35, identified as **2a** (δ(MePt) 1.57, $^2J_{PtH}$ = 84 Hz; δ(H^6) 9.62, $^3J_{PtH}$ = 18 Hz) and **2b** (δ(MePt) 1.43, $^2J_{PtH}$ = 78 Hz; δ(H^6) 9.48, $^3J_{PtH}$ = 23), respectively. For each isomer, the pyridyl nitrogen is *trans* to the methylplatinum group, as shown by the small value of the coupling constant $^3J_{PtH}$ to the *ortho* proton.[17] We were unable to separate these complexes either by crystallization or by chromatography.

Oxidative addition reactions of complex [$PtMe_2$(adpp)], 2, to give platinum(IV) derivatives

Complex **1** reacted with iodine or with alkyl halides by *trans* oxidative addition to give the organoplatinum(IV) complexes illustrated in Scheme 6. The complexes were formed as a mixture of isomers, but since the platinum(IV) complexes are stable on a silica column, it was possible to separate the isomers in some cases by column chromatography.

The complexes were initially characterized by their ^{1}H NMR and mass spectra. The iodine adduct [PtI_2Me_2(adpp)], **3**, was isolated as a yellow solid and the isomers were successfully separated. The ^{1}H NMR spectrum of the major isomer **3a** contained two methylplatinum resonances (δ(MePt) 2.50 and 2.83, each with $^2J_{PtH}$ = 74 Hz) with coupling constants $^2J_{PtH}$ characteristic for platinum(IV) complexes.[11] The ^{1}H NMR spectrum of the major isomer of [$PtIMe_3$(adpp)], **4a**, showed three equal intensity methylplatinum resonances (δ 0.83, $^2J_{PtH}$ = 74 Hz, assigned to the axial methyl group, δ 1.64, $^2J_{PtH}$ = 71 Hz, and 1.93, $^2J_{PtH}$ = 72 Hz, assigned to the equatorial methyl groups). An additional feature of complexes **5–7** is that the CH_2 protons of the ethyl or benzyl group are diastereotopic and occur as an "AB" multiplet in the ^{1}H NMR spectrum, with further coupling to the methyl protons when X = Et (Scheme 6). For example, the CH_2Pt resonances of **6a** were observed at δ 2.98 (m, 1H, $^2J_{HH}$ = 10 Hz, $^2J_{PtH}$ = 91 Hz, $PtCH^A$) and δ 3.05 (m, 1H, $^2J_{HH}$ = 10 Hz, $^2J_{PtH}$ = 90 Hz, $PtCH^B$).

The structures of complexes **6a** and **7b** were determined and are shown in Figs. 5 and 6, and each complex has the octahedral stereochemistry at platinum(IV) expected for the product of *trans* oxidative addition to isomer **1a** or **1b**, respectively. Because the ligand adpp is unsymmetrical, the complexes are chiral and the lattices contain both *C* and *A* enantiomers. In both complexes, the benzyl group is directed towards the azobenzene group, perhaps to optimize π-stacking attractions.

A summary of conformational parameters for the adpp ligand is given in Table 1. In complex **7b**, the 2-pyridyl group that is *ortho* to the azobenzene group is not coordinated and its conformation, measured by Θ1, is similar to that in the free ligand adpp, whereas the conformation of this 2-pyridyl group in **6a** is similar to that in **1a**. The 2-pyridyl group that is *meta* to the azobenzene group is always roughly coplanar with the pyridazine ring, but flipped in **7b** compared to the other compounds (Table 1). There is a large variation in the twist of the aryl groups of the azobenzene unit, Θ4, and this appears to arise from intermolecular packing forces. Complex **6a** gives the largest value of Θ4, and there is intermolec-

Scheme 3. Synthesis of the azobenzene-tagged ligand adpp.

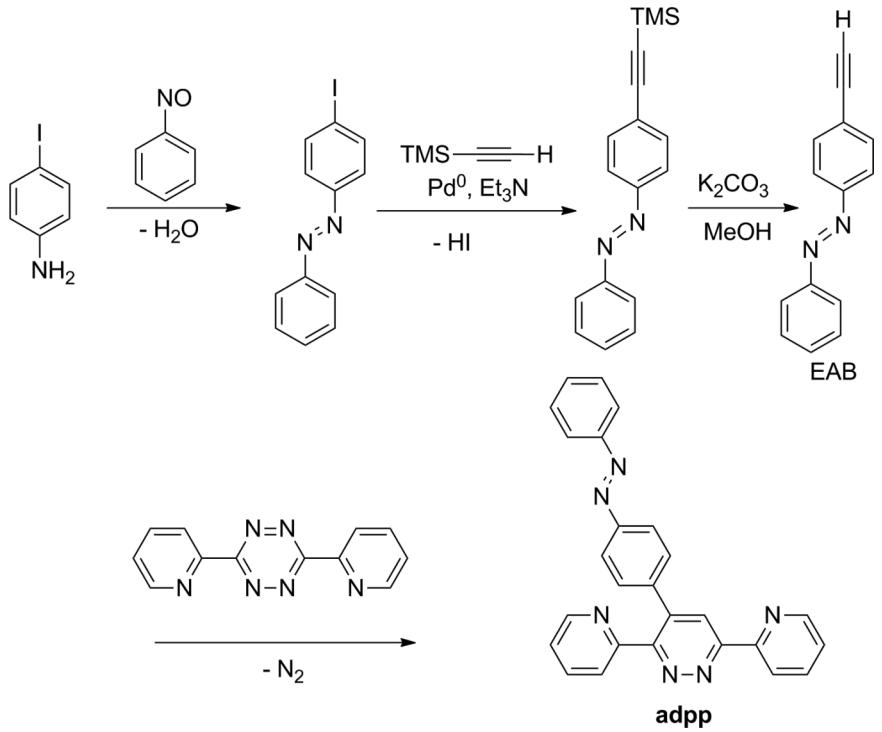

Fig. 1. Left: view of the structure of the ligand adpp; selected bond lengths (Å): N(2)–N(3) 1.3365(9), N(5)–N(6) 1.2579(9). Right: favourable hydrogen bond interactions. The twisting of the *ortho* 2-pyridyl group weakens the hydrogen bond with the pyridazine nitrogen atom.

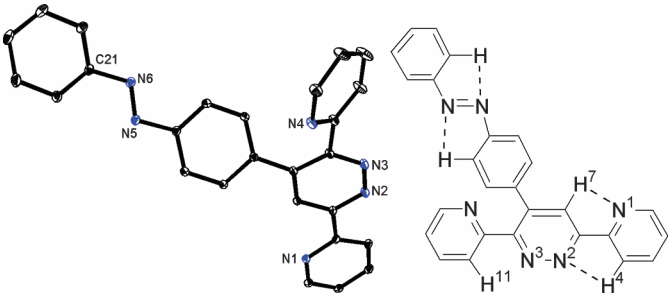

ular π-stacking between phenyl groups of neighbouring molecules.

Photoisomerization studies

The UV-visible spectra of the compounds were measured in dichloromethane solution (Table 2; Fig. 7) to investigate the effect of metal on the electronic absorption spectrum of the azobenzene unit. Both the precursor compound EAB and the free ligand adpp contain a weak n–π* band at 455 nm and a strong π–π* band at 340–341 nm, while adpp gives an extra band at 290 nm associated with the dipyridylpyridazine (dppz) group.[1–4,21, 28–32] In complex **1** (largely isomer **1a**), there is a strong band at 318 nm, assigned to the dppz transition, with a broad shoulder at approximately 350 nm, assigned to the π–π* transition, and two weak, broad overlapping peaks at approximately 430 nm, assigned to the n–π* transition, and approximately 530 nm, assigned to a metal-to-ligand charge transfer transition originating from the filled $5d_z2$ orbital of the electron-rich platinum(II) centre.[33–37] This low-energy band at approximately 530 nm in **1** was absent in the platinum(IV) complexes.

The isomerization of the azobenzene group in the compounds from the more stable *trans* to the less stable *cis* isomer was effected by irradiation using λ(irr) 365 nm, which excites primarily the π–π* transition of the *trans*-azobenzene group, while the reverse reaction occurred slowly and spontaneously at room temperature, as illustrated for the ligand adpp in Scheme 7. The reactions were monitored by UV-visible and ^{1}H NMR spectroscopy.[1–11]

The changes in UV-visible spectra on photoisomerization of adpp are illustrated in Fig. 8. The main feature is the decrease in intensity of the π–π* transition of the *trans* isomer at 340 nm, while there is a small increase in the intensity of the n–π* transition for the *cis* isomer at 441 nm. The quantum yield for photoisomerisation (Φ = 0.12) (Table 2) was very similar to that for the azobenzene standard (Φ = 0.11).[29–33] The changes were fully reversed when the sample was stored in the dark, as slow thermal isomerization back to the *trans* isomer occurred.

Changes in part of the ^{1}H NMR spectrum upon photoisomerization of adpp are shown in Fig. 9, emphasizing changes in selected resonances of the di-2-pyridylpyridazine protons. Upon illumination of the free ligand *trans*-adpp in CD_2Cl_2 with λ(irr) 365 nm for 5 min, new peaks assigned to the *cis* isomer were observed. The changes were reversed when the sample was stored in the dark.

The photoisomerization of the platinum complexes was studied in a similar way. A typical series of UV-visible spectra is shown in Fig. 10 for complex **6**. During the course of irradiation with 365 nm light, a decrease in intensity of the π–π* band of the *trans* isomer at 320 nm was observed with the growth of a band at 437 nm attributed to the n–π* band of the *cis* isomer. Keeping the irradiated sample in the dark for 1 day led to recovery of the π–π* band of the *trans* isomer, confirming that the *cis*-to-*trans* isomerization can be achieved thermally. Notably, the thermal isomerization was slower than the analogous reaction for the free ligand adpp. Figure 11 shows the recovery of intensity of the π–π* band of the *trans* isomer on warming the sample. As monitored by ^{1}H NMR spectroscopy, the irradiated sample solution contained about 25% of the *trans* and 75% of the *cis* isomer at the photostationary state. The other platinum complexes behaved similarly and data are given in Table 2. It can be seen that the quantum yields for pho-

Scheme 4. Synthesis of [$PtMe_2$(adpp)], **1**.

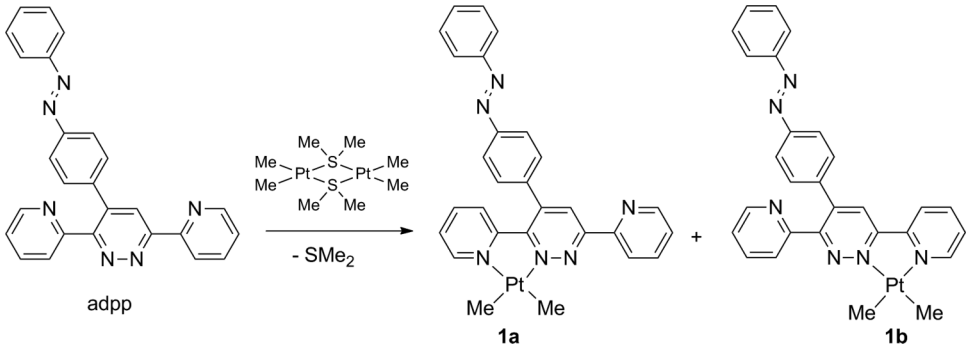

Fig. 2. ^{1}H NMR spectrum (400 MHz, chloroform-*d*) of complex **1** in the methylplatinum region. ^{195}Pt satellite peaks of the major isomer **1a** are indicated by asterisks.

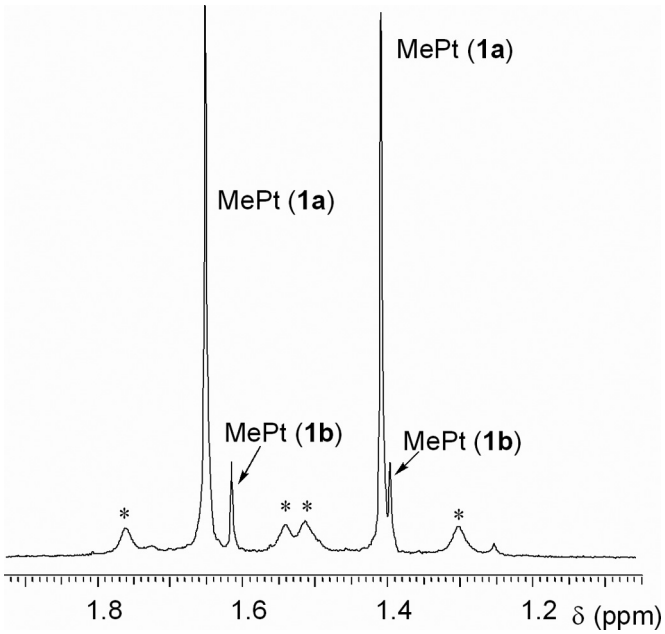

Fig. 3. View of the structure of the complex [$PtMe_2$(adpp)], **1a**. Thermal ellipsoids are at the 30% probability level and hydrogen atoms are omitted for clarity. Selected bond lengths (Å): Pt(1)–C(1) 2.038(2), Pt(1)–C(2) 2.045(3), Pt(1)–N(2) 2.076(2), Pt(1)–N(1) 2.084(19), N(2)–N(3) 1.331(3), N(5)–N(6) 1.255(3). Hydrogen bond distance Pt(1)··H(1X) 2.65 Å.

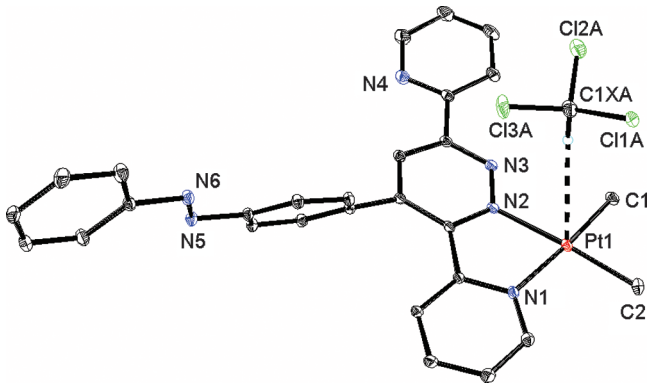

Fig. 4. The π-stacking between molecules of complex **1a**.

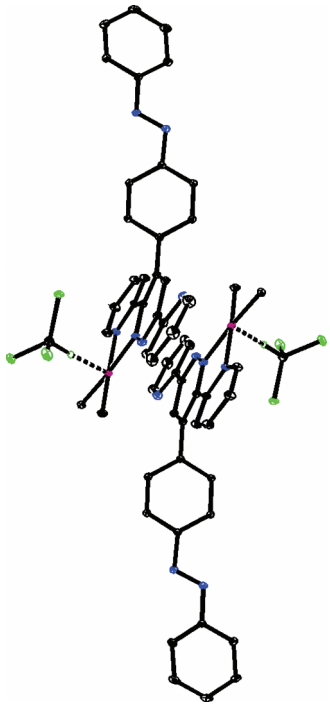

toisomerization are lower than for the ligand adpp or its precursor EAB.

Conclusions

The ligand adpp is unsymmetrical and so it can give isomeric platinum(II) complexes such as **1a** and **1b** (Scheme 4). Once formed, the isomer ratio for the complexes in solution does not change and the platinum(IV) complexes are sufficiently stable to allow separation by column chromatography. Many platinum complexes are kinetically inert, so the isomer ratio is likely to be controlled mostly by kinetic factors. To gain further insight into the thermodynamic stability of the isomers, DFT calculations (BLYP functional, double-zeta basis set, first-order scalar relativistic corrections) were carried out for the isomers of the platinum(II) complex **1** and the platinum(IV) complexes **6** and **7**, for which the structures of **1a**, **6a**, and **7b** were known (Figs. 3, 5, and 6). Typical calculated structures for **1a** and **1b** are shown in Fig. 12. For all cases, the isomer **1a**, **6a**, or **7a** was calculated to be 10–11 kJ mol^{-1} more stable than the corresponding isomer **1b**, **6b**, or **7b**, with no significant variation with oxidation state of platinum or steric effects of substituents. The observed isomer ratio of **1a**/**1b** of approximately 6, if representing an equilibrium constant,

Scheme 5. Synthesis of the complex [PtClMe(adpp)], **2.**

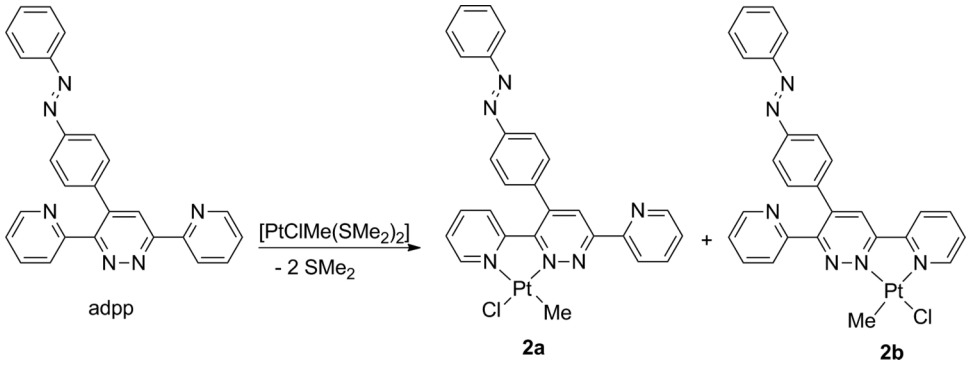

Scheme 6. Oxidative addition reactions of complex **2**.

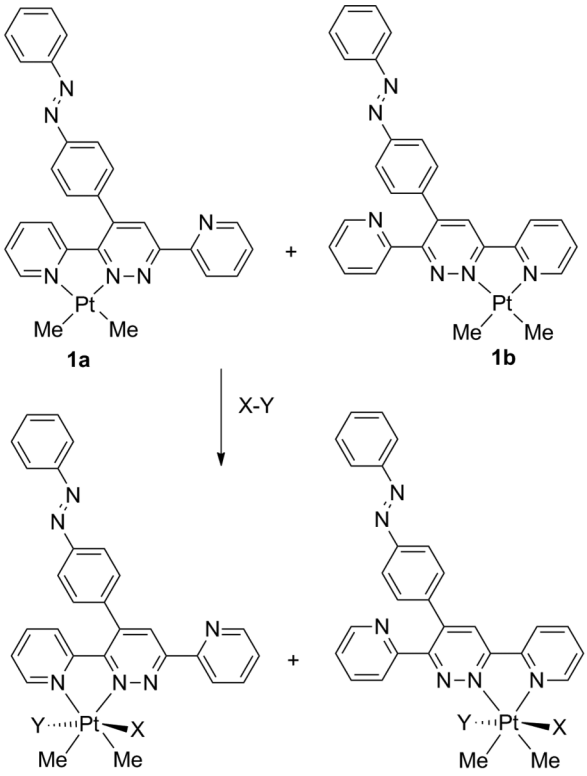

3a, X = Y = I
4a, X = Me, Y = I
5a, X = Et, Y = I
6a, X = $CH_2C_6H_4$-4-^{t}Bu, Y = Br
7a, X = $CH_2C_6H_3$-3,5-^{t}Bu$_2$, Y = Br

3b, X = Y = I
4**b**, X = Me, Y = I
5b, X = Et, Y = I
6b, X = $CH_2C_6H_4$-4-^{t}Bu, Y = Br
7b, **X =** $CH_2C_6H_3$-3,5-^{t}Bu$_2$, Y = Br

would require ΔG for the equation of Fig. 12 at 298 K of 4.5 kJ mol^{-1}, in reasonable agreement with the calculation. We conclude that both kinetic and thermodynamic factors favour the formation of isomer **1a** over **1b**.

The DFT calculations for the *cis*-azobenzene isomers, formed by photoisomerization, predict that they are about 50 kJ mol^{-1} less stable than the corresponding *trans*-azobenzene isomers. Similar values were calculated for the platinum(II) and platinum(IV) complexes studied previously as well as for the parent ligands.[10,11] Compared to the previous compounds, **A** and **B** (Scheme 2), the complexes studied here are photoisomerized more easily than **A** but less easily than **B**. This indicates that placing the azobenzene

Fig. 5. View of the structure of the complex [PtBrMe$_2$($CH_2C_6H_4$-4-*t*-Bu)(adpp)], **6a**. Ellipsoids are at the 30% probability level and hydrogen atoms were omitted for clarity. Selected bond lengths (Å): Pt(1)–C(1) 2.051(2), Pt(1)–C(2) 2.044(2), Pt(1)–C(3) 2.074(2), Pt(1)–N(1) 2.1669(17), Pt(1)–N(2) 2.1462(17), Pt(1)–Br(1) 2.6073(6), N(2)–N(3) 1.331(2), N(5)–N(6) 1.260(3).

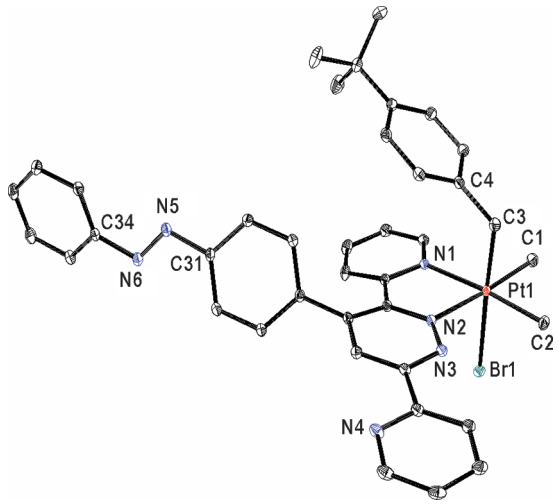

Fig. 6. View of the structure of the complex [PtBrMe$_2$($CH_2C_6H_3$-3,5-*t*-Bu$_2$)(adpp)], **7b**. Ellipsoids are at the 30% probability level and hydrogen atoms were omitted for clarity. Selected bond lengths (Å): Pt(1)–C(1) 2.044(5), Pt(1)–C(2) 2.034(5), Pt(1)–C(3) 2.091(5), Pt(1)–N(1) 2.149(4), Pt(1)–N(2) 2.141(4), Pt(1)–Br(1) 2.6037(7), N(2)–N(3) 1.333(5), N(5)–N(6) 1.175(7).

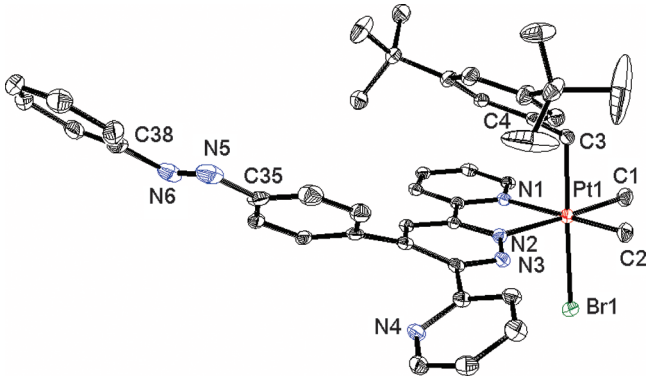

Table 1. Conformation of adpp in the free ligand and its complexes.

	adpp	**1a**	**6a**	**7b**
Θ1[a]	137	11	13	146
Θ2[a]	169	166	175	5
Θ3[a]	43	66	58	43
Θ4[b]	7	22	41	21

[a]Twist angle (°) with respect to the pyridazine ring: Θ1, 2-pyridyl group *ortho* to azobenzene; Θ2, 2-pyridyl group *meta* to azobenzene; Θ3, C_6H_4 group.

[b]Θ4, twist angle between C_6H_5 and C_6H_4 groups of azobenzene. The angles Θ1 and Θ2 are reported with respect to the ideal chelate conformation.

group farther from the platinum centre, as in **1–7** compared to **A**, leads to more efficient photochemistry but that the difference is less marked than when an insulating saturated carbon centre is placed between the platinum and azobenzene units, as in **B**.[10,11] The lower quantum yields for the platinum complexes can thus be correlated with the degree of mixing of the π–π* excited state with metal-based excited states, such as the MLCT excited states for the platinum(II) complexes studied in this work.

Experimental

All reactions were performed under nitrogen atmosphere. ^{1}H and ^{13}C NMR spectra were recorded by using Varian Mercury 400, Inova 400, and Inova 600 spectrometers, and data are reported with respect to the labeling system of Chart 1. When mixtures of isomers were present, assignments were confirmed by 2D COSY ^{1}H NMR spectroscopy and, when possible, by comparison with the NMR spectra of pure isomers. UV-visible spectra were measured using a Varian Cary 300 Bio spectrophotometer. Mass spectra were recorded using an electrospray PE-Sciex mass spectrometer (ESI-MS). DFT calculations were carried out by using the Amsterdam Density Functional program based on the BLYP functional, with double-zeta basis set and first-order scalar relativistic corrections.[38]

Photoswitching studies

For UV-visible monitoring, a sample of the complex was dissolved in dichloromethane and was irradiated in a quartz cuvette with 1 cm width at room temperature with UV light at 365 nm followed immediately by recording the absorption spectrum. For ^{1}H NMR monitoring, a sample in $CDCl_3$ or CD_2Cl_2 in an NMR tube was irradiated at room temperature at 365 nm followed by recording the spectrum.

Quantum yield determinations

A solution of the *trans* isomer of each compound in dichloromethane was illuminated with UV light at 365 nm, and the absorbance at the π–π* band maximum was recorded every 30 s. The *trans* to *cis* photoisomerization rate ν was obtained from the slope of the graph of concentration of *trans* isomer against irradiation time using azobenzene as a standard.

X-ray structure determinations

In a typical experiment, a sample was mounted on a Mitegen polyimide micromount with Paratone N oil. All X-ray measurements were made using a Bruker Kappa Axis Apex2 diffractometer at a temperature of 110 K. The frame integration was performed using SAINT.[39a] The resulting raw data were scaled and absorption corrected using a multiscan averaging of symmetry equivalent data using SADABS.[39b] The structure was solved by direct methods using the SIR2011 program.[40] The hydrogen atoms for the main molecule were introduced at idealized positions and were allowed to refine isotropically. The structural model was fit to the data using full matrix least-squares based on F^2. The structure was refined using SHELXL-2013.[41] Data are given in Table 3 (CCDC 985642, 985643, 985645, and 985646) and unusual features are described below.

The structure of the ligand adpp contained a disordered molecule of acetone of solvation. The disorder was comprised of both crystallographically imposed disorder and a general disorder, and it was successfully modeled. The structure of complex **1a** contained a disordered molecule of $CHCl_3$ of solvation that was modeled successfully. The structure of **6a** exhibited disorder of the *t*-butyl group over two sites and disorder of a molecule of CH_2Cl_2 of solvation over two sites. For this structure, there was anomalous electron density close to the platinum and bromine atoms, perhaps resulting from deficiency in the absorption correction.

4-(4-Azobenzene)-3,6-di(2-pyridyl)pyridazine, adpp

To a solution of 3,6-di(2-pyridyl)-1,2,4,5-tetrazine (1 g, 4.24 mmol) in dry toluene (40 mL) was added EAB (0.872 g, 4.24 mmol), and the reaction mixture was heated under reflux for 48 h. The solvent was removed under reduced pressure to afford the crude product as a brown solid, which was purified by column chromatography, using dichloromethane–hexane (15%:85%) as eluent, and was isolated as an orange powder. Yield 63% (1.1 g). NMR in $CDCl_3$, *trans*-adpp, δ(^{1}H): 7.32 (m, 1H, H^{5C}), 7.46 (m, 3H, H^{5A}, H^{mD}), 7.53 (m, 3H, H^{mE} and H^{pE}), 7.85 (m, 1H, H^{4C}), 7.90 (d, 2H, $^3J_{HH}$ = 8 Hz, H^{oD}), 7.94 (m, 3H, H^{4A} and H^{oE}), 8.04 (d, 1H, $^3J_{HH}$ = 8 Hz, H^{3C}), 8.48 (d, 1H, $^3J_{HH}$ = 5 Hz, H^{6C}), 8.74 (s, 1H, H^{5B}), 8.75 (d, 1H, $^3J_{HH}$ = 5 Hz, H^{6A}), 8.84 (d, 1H, $^3J_{HH}$ = 8 Hz, H^{3A}); δ(^{13}C): 158.0, 157.7, 155.5, 153.2, 152.5, 152.1, 149.5, 149.1, 139.71, 137.2, 136.7, 131.2, 129.7, 129.1, 125.5, 124.3, 123.5, 122.9, 121.9. HRMS (ESI) calcd. for $C_{26}H_{18}N_6$ $[M]^+$: 414.159; found: 414.159. Single crystals of adpp were grown by slow diffusion of *n*-pentane into a solution of the ligand dissolved in acetone. After photolysis, NMR in $CDCl_3$, *cis*-adpp, δ(^{1}H): 6.81 (m, 2H, H^{mE}), 6.87 (d, 2H, $^3J_{HH}$ = 8 Hz, H^{mD}), 7.16 (d, 2H, $^3J_{HH}$ = 8 Hz, H^{oD}), 7.20 (t, 1H, $^3J_{HH}$ = 8 Hz, H^{pE}), 7.25 (m, 1H, H^{5C}), 7.46 (m, 1H, H^{5A}), 7.30 (m, 2H, $^3J_{HH}$ = 8 Hz, H^{oE}), 7.82 (m, 1H, H^{4C}), 7.93 (m, 1H, H^{4A}), 7.96 (d, 1H, $^3J_{HH}$ = 8 Hz, H^{3C}), 8.39 (d, 1H, $^3J_{HH}$ = 5 Hz, H^{6C}), 8.61 (s, 1H, H^{5B}), 8.73 (d, 1H, $^3J_{HH}$ = 5 Hz, H^{6A}), 8.80 (d, 1H, $^3J_{HH}$ = 8 Hz, H^{3A}).

[PtMe$_2$(adpp)], 1

To a stirred solution of adpp (0.3 g, 0.724 mmol) in toluene (20 mL) was added $[Pt_2Me_4(\mu\text{-}SMe_2)_2]$ (0.208 g, 0.362 mmol). The solution colour rapidly changed from orange to red with precipitation of a red solid. The reaction mixture was stirred for 1 h for reaction completion. The solid complex was collected by filtration, washed with ether (3 × 2 mL) and pentane (3 × 2 mL), and dried under high vacuum. Yield 82% (0.38 g). NMR in $CDCl_3$, **1a**, δ(^{1}H): 1.41 (s, 3H, $^2J_{PtH}$ = 87 Hz, PtMe), 1.65 (s, 3H, $^2J_{PtH}$ = 87 Hz, PtMe), 7.26 (m, 3H, H^{5C}, H^{mE}), 7.31 (m, 1H, H^{5A}), 7.47 (m, 8H, H^{3C}, H^{4A}, H^{oE}, H^{mD}, H^{4C} and H^{pE}), 7.66 (dt, 1H, $^3J_{HH}$ = 6 Hz, H^{6C}), 7.91 (d, 2H, $^3J_{HH}$ = 8 Hz, H^{oD}), 8.14 (s, 1H, H^{5B}), 8.21 (m, 1H, H^{3A}), 8.32 (d, 1H, $^3J_{HH}$ = 5 Hz, $^3J_{PtH}$ = 23 Hz, H^{6A}); **1b**, δ(^{1}H): 1.40 (s, 3H, $^2J_{PtH}$ = 88 Hz, Pt-Me), 1.62 (s, 3H, $^2J_{PtH}$ = 88 Hz, Pt-Me), 7.17 (m, 1H, H^{5A}), 7.23 (m, 1H, H^{5C}), 7.59 (m, 5H, H^{mD}, H^{mE} and H^{pE}), 7.72 (m, 1H, H^{4A}), 7.97 (m, 1H, H^{4C}), 8.0 (m, 3H, H^{3A}, H^{oE}), 8.10 (d, 2H, $^3J_{HH}$ = 8 Hz, H^{oD}), 8.74 (d, 1H, $^3J_{HH}$ = 6 Hz, H^{6A}), 8.90 (d, 1H, $^3J_{HH}$ = 8 Hz, H^{3C}), 8.99 (s, 1H, H^{5B}), 9.40 (d, 1H, $^3J_{HH}$ = 6 Hz, $^3J_{PtH}$ = 23 Hz, H^{6C}). Single crystals were grown by slow diffusion of *n*-pentane into a solution of the compound dissolved in chloroform.

[PtClMe(adpp)], 2

To a stirred solution of the ligand (4-adppn) (0.1 g, 0.241 mmol) in acetone (10 mL) was added trans $[Pt_2ClMe(SMe_2)_2]$ (0.089 g, 0.241 mmol). The solution colour immediately changed to red with precipitation of a red solid. The reaction mixture was stirred at room temperature for 1 h. The solid complex was collected by filtration, washed with ether (3 × 2 mL) and pentane (3 × 2 mL), and dried under high vacuum. Yield 89% (0.146 g). NMR in CD_2Cl_2, **2a**, δ(^{1}H): 1.57 (s, 3H, $^2J_{PtH}$ = 84 Hz, Pt-Me), 7.49 (m, 1H, H^{5C}), 7.54 (m, 6H, H^{mE}, H^{mD}, H^{pE} and H^{5A}), 7.71 (m, 1H, H^{4C}), 7.95 (m, 6H, H^{4A}, H^{3C}, H^{oD}

Table 2. Absorption maxima (nm) for the UV-visible bands associated primarily with the *trans* and *cis* azobenzene group and quantum yields for photoisomerization of the *trans* to the *cis* isomer.

	AB[a]	EAB[b]	adpp	**1**	**2**	**3**	**4**	**5**	**6**	**7**
trans										
$\pi-\pi^*$	320	340	341	318	318	319	318	318	320	319
$n-\pi^*$	450	455	455	448	445	446	448	429	448	447
$10^{-5}\varepsilon(\pi-\pi^*)$[c]			6.0	6.8	9.9	2.2	7.8		9.7	9.7
$10^{-5}\ \varepsilon(365)$[d]			3.0	3.1	6.1	1.1	4.2		3.7	4.0
cis										
$\pi-\pi^*$	280	267	266	NR[f]	NR[f]	NR[f]	265	265	266	263
$n-\pi^*$	440	442	445	445	440	441	444	425	448	443
Φ[e]	0.11	0.13	0.12	0.077	0.089	0.095	0.092	0.087	0.089	0.093

[a]AB = azobenzene.
[b]EAB = 4-ethynylazobenzene.
[c]Extinction coefficient (M^{-1} cm^{-1}) at absorption maximum of the $\pi-\pi^*$ transition.
[d]Extinction coefficient (M^{-1} cm^{-1}) at irradiation wavelength of 365 nm.
[e]Quantum yield for *trans–cis* isomerization with λ(irr) 365 nm in dichloromethane.
[f]Not resolved.

Fig. 7. UV-visible spectra of 4-ethynylazobenzene, EAB, free ligand adpp, and complex **1** in dichloromethane.

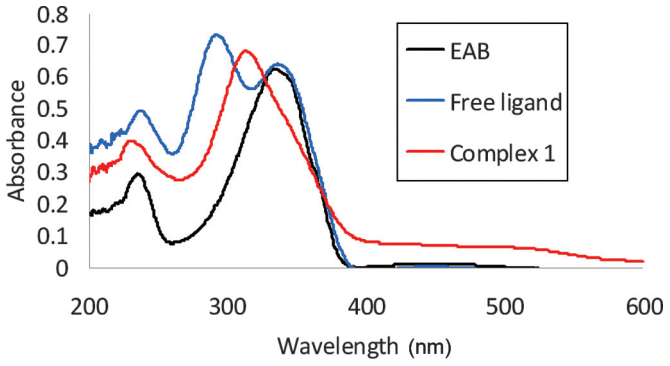

Scheme 7. Photoisomerization of the azobenzene-tagged ligand.

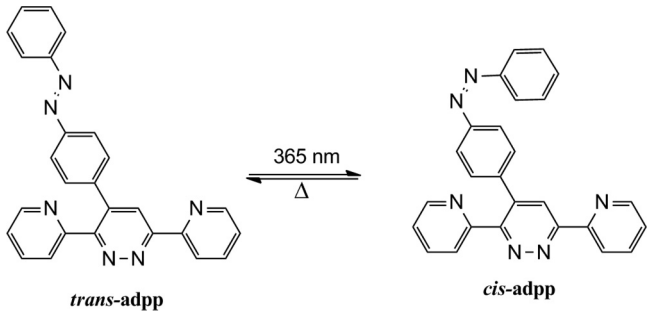

and H^{oE}), 8.20 (s, 1H, H^{5B}), 8.21 (m, 1H, H^{6C}), 8.41 (d, 1H, $^3J_{HH}$ = 6 Hz, H^{3A}), 9.62 (d, 1H, $^3J_{HH}$ = 6 Hz, $^3J_{PtH}$ = 18 Hz, H^{6A}); **2b**, δ(^{1}H): 1.43 (s, 3H, $^2J_{PtH}$ = 78 Hz, Pt-Me), 7.37 (m, 1H, H^{5A}), 7.25 (d, 2H, $^3J_{HH}$ = 8 Hz, H^{mD}), 7.60 (m, 4H, H^{5C}, H^{mE} and H^{pE}), 7.73 (dt, 1H, $^3J_{HH}$ = 8 Hz, H^{4A}), 8.01 (m, 4H, H^{4C}, H^{3A} and H^{oD}), 8.12 (d, 2H, $^3J_{HH}$ = 8 Hz, H^{oE}), 8.70 (d, 1H, $^3J_{HH}$ = 6 Hz, H^{6A}), 8.75 (d, 1H, $^3J_{HH}$ = 8 Hz, H^{3C}), 9.05 (s, 1H, H^{5B}), 9.48 (d, 1H, $^3J_{HH}$ = 6 Hz, $^3J_{PtH}$ = 23 Hz, H^{6C}). HRMS (ESI) calcd. for $C_{27}H_{21}N_6NaPt$ $[M]^+$: 682.1063; found: 682.1056.

[PtI_2Me_2(adpp)], 3

To a solution of complex **1** (0.05 g, 0.078 mmol) in acetone (15 mL) was added excess iodine. After 10 min, the colour of the solution had changed from red to yellow with precipitation of a yellow solid. The mixture was stirred for 1 h and then the solid was isolated by filtration, washed with ether (3 × 2 mL) and pentane (3 × 2 mL), and dried under vacuum. Yield 85% (0.06 g). The complex was purified by column chromatography using acetone–hexanes (15%:85%) as eluent. NMR in $CDCl_3$, **3a**, δ(^{1}H): 2.51 (s, 3H,

Fig. 8. Change in the UV-visible spectrum upon photoisomerization of the ligand adpp in dichloromethane with λ(irr) 365 nm (*a*) before irradiation and (*b*) after 2 min of irradiation.

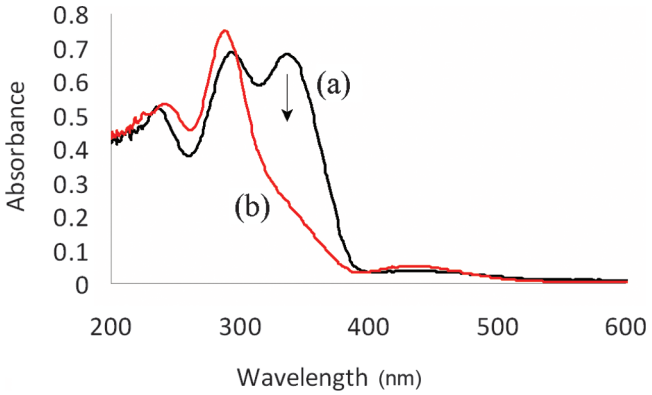

Fig. 9. ^{1}H NMR spectrum, in the region from δ 8.3 to 8.9, of the ligand adpp (*a*) before irradiation (*trans* isomer only) and (*b*) after photolysis for 5 min with λ(irr) 365 nm (both *trans* and *cis* isomers present).

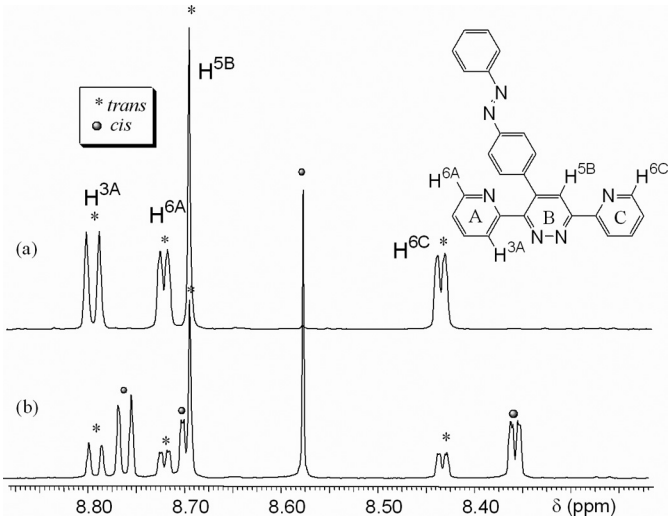

$^2J_{PtH}$ = 74 Hz, Pt-Me), 2.83 (s, 3H, $^2J_{PtH}$ = 74 Hz, Pt-Me), 7.48 (d, 2H, $^3J_{HH}$ = 8 Hz, H^{mD}), 7.53 (m, 1H, H^{5C}), 7.59 (m, 3H, H^{mE} and H^{5A}), 7.68 (m, 1H, H^{pE}), 7.72 (d, 2H, $^3J_{HH}$ = 8 Hz, H^{oD}), 7.98 (m, 1H, H^{4C}), 8.02 (m, 2H, H^{3C} and H^{4A}), 8.13 (d, 2H, $^3J_{HH}$ = 8 Hz, H^{oE}), 8.77 (d, 1H, $^3J_{HH}$ = 6 Hz, H^{6C}), 8.84 (s, 1H, H^{5B}), 8.91(d, 1H, $^3J_{HH}$ = 8 Hz, H^{3A}), 9.12 (d, 1H,

Fig. 10. UV-visible spectral changes upon photolysis of complex **6** at 365 nm in dichloromethane.

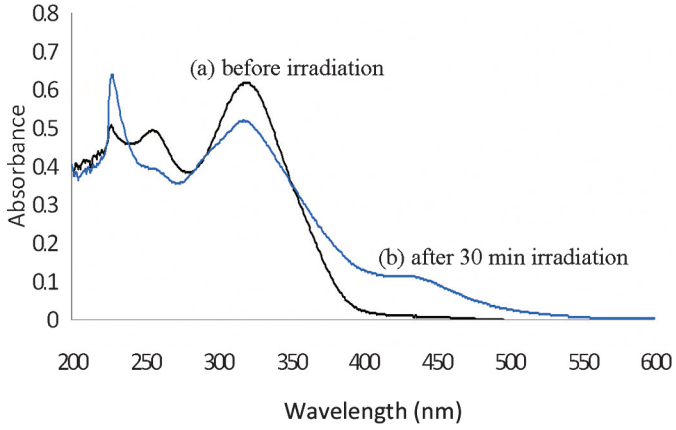

Fig. 11. Recovery of the trans $\pi-\pi^*$ band at maximum absorbance 319 nm of complex **7** on heating at a rate of 2 °C min^{-1}.

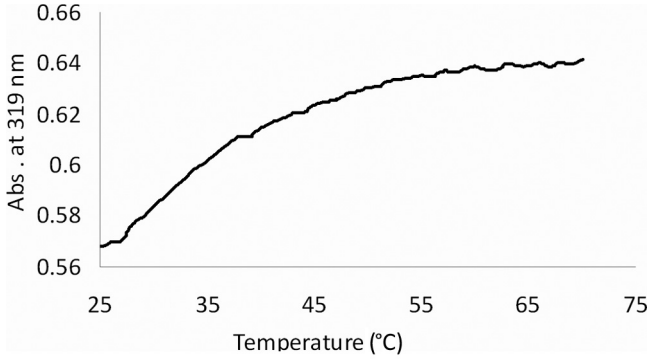

Fig. 12. Calculated structures of complexes **1a** and **1b**.

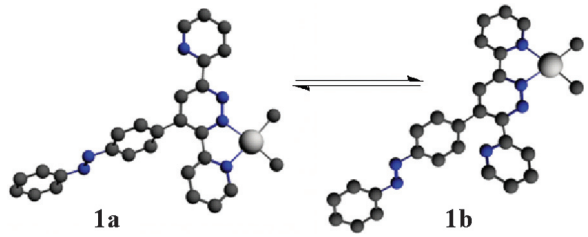

$^3J_{HH}$ = 6 Hz, $^3J_{PtH}$ = 23 Hz, H^{6A}); **3b**, δ(^{1}H): 2.48 (s, 3H, $^2J_{PtH}$ = 74 Hz, Pt-Me), δ 2.81 (s, 3H, $^2J_{PtH}$ = 74 Hz, Pt-Me), 7.37 (m, 1H, H^{5A}), 7.47 (d, 2H, $^3J_{HH}$ = 7 Hz, H^{mD}), 7.55 (m, 3H, Hm^{mE} and H^{pE}), 7.82 (m, 1H, H^{5C}), 7.98 (m, 5H, H^{4C}, H^{oE} and H^{oD}), 8.16 (m, 1H, H^{4C}), 8.39 (m, 3H, H^{3C}, H^{6A} and H^{3A}), 8.44 (s, 1H, H^{5B}), 9.10 (d, 1H, $^3J_{HH}$ = 6 Hz, $^3J_{PtH}$ = 23 Hz, H^{6C}). HRMS (ESI) calcd. for $C_{28}H_{24}IN_6$ Pt[M-I]$^+$: 766.0755; found: 766.0955.

[PtIMe$_3$(adpp)], 4

To a solution of complex **1** (0.05 g, 0.078 mmol) in acetone (15 mL) was added methyl iodide (0.02 mL). The mixture was stirred for 1 h and then the yellow precipitate of the product was collected by filtration, washed with ether (3 × 2 mL) and pentane (3 × 2 mL), and dried under high vacuum. Yield 94% (0.056 g). The complex was purified via column chromatography technique using dichloromethane–hexanes (10%:90%) as eluent. NMR in $CDCl_3$, **4a**, δ(^{1}H): 0.83 (s, 3H, $^2J_{PtH}$ = 74 Hz, Pt-Me), 1.64 (s, 3H, $^2J_{PtH}$ = 71 Hz, Pt-Me), 1.93 (s, 3H, $^2J_{PtH}$ = 72 Hz, Pt-Me), 7.52 (m, 1H, H^{5C}), 7.57(m, 5H, H^{mE}, H^{pE}, H^{4C} and H^{5A}), 7.69 (m, 1H, H^{4A}), 7.72 (d, 2H, $^3J_{HH}$ = 8 Hz, H^{mD}), 7.97 (m, 3H, H^{3C} and H^{oD}), 8.12 (d, 2H, $^3J_{HH}$ = 8 Hz, H^{oE}), 8.76 (d, 1H, $^3J_{HH}$ = 8 Hz, H^{6C}), 8.84 (m, 1H, H^{5B}), 8.92 (d, 1H, $^3J_{HH}$ = 7 Hz, H^{3A}), 9.10 (d, 1H, $^3J_{HH}$ = 6 Hz, $^3J_{PtH}$ = 18 Hz, H^{6A}), **4b**, δ(^{1}H): 0.77 (s, 3H, $^2J_{PtH}$ = 74 Hz, Pt-Me), 1.51 (s, 3H, $^2J_{PtH}$ = 71 Hz, Pt-Me), 1.77 (s, 3H, $^2J_{PtH}$ = 71 Hz, Pt-Me), 7.37 (m, 1H, H^{5A}), 7.45 (d, 2H, $^3J_{HH}$ = 9 Hz, H^{mD}), 7.56 (m, 3H, H^{mE} and H^{pE}), 7.77 (m, 1H, H^{5C}), 7.93 (m, 5H, H^{4A}, H^{oE} and H^{oD}), 8.17 (m, 1H, H^{4C}), 8.22 (d, 1H, $^3J_{HH}$ = 8 Hz, H^{3A}), 8.41 (m, 2H, H^{3C} and H^{6A}), 8.47 (s, 1H, H^{5B}), 9.07 (d, 1H, $^3J_{HH}$ = 6 Hz, $^3J_{PtH}$ = 18 Hz, H^{6C}). HRMS (ESI) calcd. for $C_{29}H_{27}N_6NaPt[M]^+$: 804.0887; found: 804.0882.

[PtIMe$_2$Et(adpp)], 5

This was prepared in a similar way but using EtI instead of MeI. Yield 92%. (0.057 g). NMR in $CDCl_3$, **5a**, δ(^{1}H): 0.30 (t, 3H, $^3J_{PtH}$ = 59 Hz, $^2J_{HH}$ = 7 Hz, PtCH$_2$*Me*), 0.89 (m, 1H, $^2J_{PtH}$ = 69 Hz, Pt-CH^A), 0.94 (m, 1H, $^2J_{PtH}$ = 68 Hz, Pt-CH^B), 1.57 (s, 3H, $^2J_{PtH}$ = 72 Hz, Pt-Me), 1.88 (s, 3H, $^2J_{PtH}$ = 72 Hz, Pt-Me), 7.47 (m, 2H, H^{5C} and H^{pE}), 7.53 (m, 1H, H^{5A}), 7.72 (m, 3H, H^{4C} and H^{mE}), 7.97 (m, 3H, H^{4A}and H^{mD}), 8.02 (m, 2H, H^{oD}), 8.11 (d, 2H, $^3J_{HH}$ = 9 Hz, H^{oE}), 8.38 (dt, 1H, $^3J_{HH}$ = 8 Hz, H^{3C}), 8.76 (d, 1H, $^3J_{HH}$ = 8 Hz, H^{6C}), 8.86 (s, 1H, H^{5B}), 8.91 (d, 1H, $^3J_{HH}$ = 7 Hz, H^{3A}), 9.06 (d, 1H,$^3J_{HH}$ = 6 Hz, $^3J_{PtH}$ = 19 Hz, H^{6A}); **5b**, δ(^{1}H): 0.21 (t, 3H, $^3J_{PtH}$ = 59 Hz, $^2J_{HH}$ = 7 Hz, PtCH$_2$*Me*), 0.79 (m, 1H, $^2J_{PtH}$ = 69 Hz, Pt-CH^A) 0.84 (m, 1H, $^2J_{PtH}$ = 68 Hz, Pt-CH^B), 1.55 (s, 3H, $^2J_{PtH}$ = 72 Hz, Pt-Me), 1.84 (s, 3H, $^2J_{PtH}$ = 72 Hz, Pt-Me), 7.34 (m, 1H, H^{5A}), 7.43 (d, 2H, $^3J_{HH}$ = 9 Hz, H^{mD}), 7.47 (m, 3H, H^{mE} and H^{pE}), 7.77 (m, 1H, H^{5C}), 7.93 (m, 4H, H^{oE} and H^{oD}), 7.80 (m, 1H, H^{4A}), 8.20 (m, 1H, H^{4C}), 8.22 (d, 1H, $^3J_{HH}$ = 8 Hz, H^{3A}), 8.36 (d, 1H, $^3J_{HH}$ = 7 Hz, H^{3C}), 8.38 (d, 1H, $^3J_{HH}$ = 7 Hz, H^{6A}), 8.40 (s, 1H, H^{5B}), 9.12 (d, 1H, $^3J_{HH}$ = 6 Hz, $^3J_{PtH}$ = 18 Hz, H^{6C}). HRMS (ESI) calcd. for $C_{30}H_{29}IN_6NaPt[M]^+$: 818.1046; found: 818.1038.

[PtBrMe$_2$(CH$_2$C$_6$H$_4$-4-*t*-Bu) (4-adppn)], 6

To a solution of complex **1** (0.04 g, 0.063 mmol) in acetone (15 mL) was added 4-*t*-butylbenzyl bromide (0.014 g, 0.063 mmol). The mixture was stirred at room temperature for 1 h and then the precipitated yellow solid was collected by filtration and washed with ether (3 × 2 mL) and pentane (3 × 2 mL) and dried under high vacuum. Yield 82% (0.044 g). The product was purified by column chromatography purification using acetone–hexanes (10%:90%) as eluent. NMR in $CDCl_3$, **6a**, δ(^{1}H): 0.94 (s, 9H, *t*-Bu), 1.59 (s, 3H, $^2J_{PtH}$ = 71 Hz, Pt-Me), 1.97 (s, 3H, $^2J_{PtH}$ = 71 Hz, Pt-Me), 2.98 (m, 1H, $^2J_{HH}$ = 10 Hz, $^2J_{PtH}$ = 91 Hz, Pt-CH^A), 3.05 (m, 1H, $^2J_{HH}$ = 10 Hz, $^2J_{PtH}$ = 90 Hz, Pt-CH^B), 6.48 (d, 2H, $^3J_{HH}$ = 3 Hz, Bn-H$^{o''}$), 6.66 (d, 2H, $^3J_{HH}$ = 8 Hz, H^{mD}), 7.24 (dt, 2H, $^3J_{HH}$ = 3 Hz, Bn-H$^{m''}$), 7.59 (m, 5H, H^{mE}, H^{pE}, H^{5C} and H^{5A}), 7.95(t, 1H, $^3J_{HH}$ = 8 Hz, H^{4C}), 8.01 (m, 4H, H^{4A}, H^{oD} and H^{3C}), 8.10 (d, 2H, $^3J_{HH}$ = 7 Hz, H^{oE}), 8.62 (s, 1H, H^{5B}), 8.74 (d, 1H, $^3J_{HH}$ = 8 Hz, H^{6C}), 8.83 (m, 1H, H^{3A}), 8.88 (d, 1H, $^3J_{HH}$ = 6 Hz, $^3J_{PtH}$ = 18 Hz, H^{6A}). HRMS (ESI) calcd. for $[C_{39}H_{39}BrN_6NaPt]^+$: 888.1958; found: 888.1959. Single crystals of complex **6a** were grown by slow diffusion of *n*-pentane into a solution of the compound dissolved in dichloromethane.

[PtBrMe$_2$(CH$_2$C$_6$H$_4$-3,5-*t*-Bu$_2$)(adpp)], 7

This was prepared in a similar way but using 3,5-di-*t*-butylbenzyl bromide. Yield 80% (0.046 g). The product was purified by column chromatography using dichloromethane–hexanes (20%:80%) as eluent. NMR in CD_2Cl_2, **7a**, δ(^{1}H): 0.96 (s, 18H, *t*-Bu), 1.58 (s, 3H, $^2J_{PtH}$ = 71 Hz, Pt-Me), 1.87 (s, 3H, $^2J_{PtH}$ = 71 Hz, Pt-Me), 2.99 (m, 1H, $^2J_{HH}$ = 11 Hz, $^2J_{PtH}$ = 91 Hz, Pt-CH^A), 3.11 (m, 1H, $^2J_{HH}$ = 11 Hz, $^2J_{PtH}$ = 90 Hz, Pt-CH^B), 6.35 (d, 2H, $^4J_{HH}$ = 3 Hz, Bn-H^o), 6.89 (t, 1H, $^4J_{HH}$ = 3 Hz, Bn-H^p), 7.47(m, 1H, H^{5C}), 7.53(m, 1H, H^{5A}), 7.55 (m, 3H, H^{mE} and H^{pE}), 7.58 (m, 3 H, H^{mD} and H^{4C}), 7.99 (d, 2H, $^3J_{HH}$ = 8 Hz, H^{oD}), 8.02 (m, 3 H, H^{4A} and H^{oE}), 8.05 (m, 2H, H^{6C} and H^{3C}), 8.76 (s, 1H, H^{5B}), 8.77 (d, 1H, $^3J_{HH}$ = 7 Hz, H^{3A}), 8.91 (d, 1H, $^3J_{HH}$ = 6 Hz, $^3J_{PtH}$ = 18 Hz, H^{6A}); **7b**, δ(^{1}H): 1.03 (s, 18H, *t*-Bu), 1.55 (s, 3H, $^2J_{PtH}$ = 71 Hz, Pt-Me), 1.79 (s, 3H, $^2J_{PtH}$ = 71 Hz, Pt-Me), 3.02 (m, 1H, $^2J_{HH}$ = 11 Hz, $^2J_{PtH}$ = 91 Hz, Pt-CH^A), 3.10 (m, 1H, $^2J_{HH}$ = 11 Hz, $^2J_{PtH}$ = 90 Hz, Pt-CH^B), 6.33 (d, 2H, $^4J_{HH}$ = 2 Hz, Bn-H^o), 7.23 (d, 2H, $^3J_{HH}$ = 8 Hz, H^{mD}), 7.43

Chart 1. NMR labeling scheme for selected compounds.

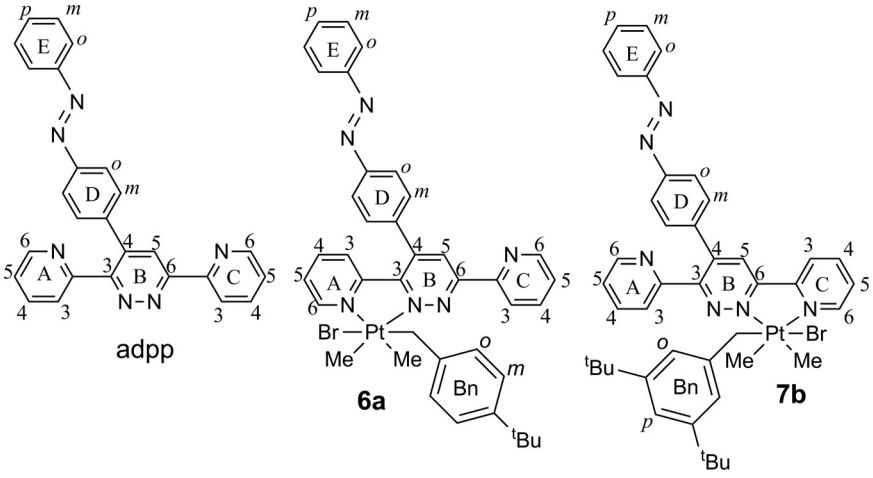

Table 3. Crystal and refinement data.

Compound	adpp $0.5Me_2CO$	**1a** $CHCl_3$	**6a** CH_2Cl_2	**7b**
Formula	$C_{27.5}H_{21}N_6O_{0.5}$	$C_{29}H_{25}Cl_3N_6Pt$	$C_{40}H_{41}BrCl_2N_6Pt$	$C_{43}H_{44}BrN_6Pt$
Formula weight (g/mol)	443.50	758.99	951.69	919.84
Colour/habit	Red prism	Red prism	Orange prism	Orange prism
Crystal system	Monoclinic	Monoclinic	Triclinic	Monoclinic
Space group	*C*2/*c*	$P2_1/c$	*P*1	*C*2/*c*
T (K)	110	110	110	110
a (Å)	31.968(9)	10.746(3)	10.762(3)	22.690(7)
b (Å)	7.0483(19)	15.813(3)	12.997(3)	15.654(5)
c (Å)	19.806(5)	16.713(4)	15.367(5)	22.617(7)
α (°)	90	90	70.860(6)	90
β (°)	94.121(5)	94.986(8)	72.847(14)	103.919(7)
γ (°)	90	90	73.649(7)	90
V (Å^3)	4451(2)	2829.3(11)	1899.3(9)	7797(4)
Z	8	4	2	8
ρ (calcd.) (g cm^{-1})	1.324	1.782	1.664	1.567
λ (Å) (MoKα)	0.71073	0.71073	0.71073	0.71073
μ (cm^{-1})	0.083	5.274	4.924	4.662
Reflections	10860	20743	23463	11017
Parameters	430	383	509	468
R_1 ($I > 2\sigma(I)$)	0.0493	0.0453	0.0383	0.0455
wR_2 (all data)	0.1483	0.0921	0.0774	0.1104

(d, 2H, $^3J_{HH}$ = 8 Hz, H^{mE}), 7.49 (t, 1H, $^4J_{HH}$ = 2 Hz, Bn-H^p), 7.55 (m, 3H, H^{pE},H^{5A} and H^{5C}), 7.95 (m, 1H, H^{4A}), 7.94 (m, 2H, H^{4C} and H^{3A}), 7.97 (d, 2H, $^3J_{HH}$ = 8 Hz, H^{oD}), 8.01 (m, 3H, H^{oE} and H^{3C}), 8.10 (d, 1H, $^3J_{HH}$ = 8 Hz, H^{6A}), 8.28 (s, 1H, H^{5B}), 8.87 (d, 1H, $^3J_{HH}$ = 6 Hz, $^3J_{PtH}$ = 18 Hz, H^{6C}). HRMS (ESI) calcd. for $C_{43}H_{47}BrN_6NaPt[M]^+$: 944.2578; found: 944.2582. Single crystals of complex **7b** were grown by slow diffusion of *n*-pentane into a solution of the compound dissolved in a mixture of equal volumes of dichloromethane and chloroform.

Supplementary material

Supplementary material is available with the article through the journal Web site at http://nrcresearchpress.com/doi/suppl/10.1139/cjc-2013-0588. Crystallographic data for the complexes are available in CIF format (CCDC 985642, 985643, 985645, and 985646).

Acknowledgement

We thank the NSERC (Canada) for financial support.

References

(1) Beharry, A. A.; Woolley, G. A. *Chem. Soc. Rev.* **2011**, *40*, 4422. doi:10.1039/c1cs15023e.
(2) Bandara, H. M. D.; Burdette, S. C. *Chem. Soc. Rev.* **2012**, *41*, 1809. doi:10.1039/c1cs15179g.
(3) Bohner, S. R.; Kruger, M.; Oesterhelt, D.; Moroder, L.; Nagele, T.; Wachtveitl, J. *J. Photochem. Photobiol. A* **1997**, *105*, 235. doi:10.1016/S1010-6030(96)04497-8.
(4) Fissi, A.; Pieroni, O.; Balestreri, E.; Amato, C. *Macromolecules* **1996**, *29*, 4680. doi:10.1021/ma960280w.
(5) Segorra-Maset, M. D.; van Leeuwen, P. W. N. M.; Freixa, Z. *Eur. J. Inorg. Chem.* 2010, 2075. doi:10.1002/ejic.201000063.
(6) Sakamoto, R.; Kume, S.; Sugimoto, M.; Nishihara, H. *Chem. Eur. J.* **2009**, *15*, 1429. doi:10.1002/chem.200801593.
(7) Marchi, E.; Baroncini, M.; Bergamini, G.; van Heyst, J.; Vogtle, F.; Ceroni, P. *J. Am. Chem. Soc.* **2012**, *134*, 15277. doi:10.1021/ja307522f.
(8) Bardaji, M.; Barrio, M.; Espinet, P. *Dalton Trans.* **2011**, *40*, 2570. doi:10.1039/c0dt01167c.
(9) Tang, H.-S.; Zhu, N.; Yam, V. W.W. *Organometallics* **2007**, *26*, 22. doi:10.1021/om0609719.
(10) Moustafa, M. E.; McCready, M. S.; Puddephatt, R. J. *Organometallics* **2012**, *31*, 6262. doi:10.1021/om3005405.
(11) Moustafa, M. E.; McCready, M. S.; Puddephatt, R. J. *Organometallics* **2013**, *32*, 2552. doi:10.1021/om4000314.
(12) Mastropietro, T.F.; Marino, N.; Armentano, D.; De Munno, g.; Yuste, C.; Lloret, F.; Julve, M. *Cryst. Growth Des.* **2013**, *13*, 270. doi:10.1021/cg301415p.
(13) Baxter, P. N.W.; Lehn, J.-M; Kneisel, Fenske, B. O.D. *Angew. Chem. Int. Ed. Engl.* **1997**, *36*, 1978. doi:10.1002/anie.199719781.
(14) Weissbuch, I.; Baxter, P. N.W.; Kuzmenko, I.; Cohen, H.; Cohen, S.; Kjaer, K.; Howes, P. B.; Als-Nielsen, J.; Lehn, J.-M.; Leiserowitz, L.; Lahav, M. *Chem. Eur. J.*

2000, *6*, 725. doi:10.1002/(SICI)1521-3765(20000218)6:4<725::AID-CHEM725>3.0.CO;2-E.
(15) Ghumaan, S.; Sarkar, B.; Patra, S.; Parimal, K.; Slageren, J.; Fiedler, J.; Kaim, W.; Lahiri, G. K. *Dalton Trans.* 2005, 706. doi:10.1039/B417530A.
(16) Denti, G.; Sabatino, L.; De Rosa, G.; Bartolotta, A.; Di Marco, G.; Ricevuto, V.; Campagna, S. *Inorg. Chem.* **1989**, *28*, 3309. doi:10.1021/ic00316a012.
(17) McCready, M. S.; Puddephatt, R. J. *Dalton Trans.* **2012**, *41*, 12378. doi:10.1039/c2dt31584j.
(18) Ghedini, M.; Longeri, M.; Neve, F. *Inorg. Chim. Acta* **1987**, *132*, 223. doi:10.1016/S0020-1693(00)81746-6.
(19) Ghedini, M.; Neve, F.; Longeri, M.; Bruno, M. *Inorg. Chim. Acta* **1988**, *149*, 131. doi:10.1016/S0020-1693(00)90579-6.
(20) Constable, E. C.; Housecroft, C. E.; Neuburger, M.; Reymann, S.; Schaffner, S. *Chem. Commun.* 2004, 1056. doi:10.1039/B402376E.
(21) Hoogenboom, R.; Kickelbick, G.; Schubert, U. S. *Eur. J. Org. Chem.* 2003, 4887. doi:10.1002/ejoc.200300505.
(22) Yu, B.-C.; Shirai, Y.; Tour, J. M. *Tetrahedron* **2006**, *62*, 10303. doi:10.1016/j.tet.2006.08.069.
(23) Shirai, Y.; Sasaki, T.; Guerrero, J. M.; Tour, J. M.; Hodge, P.; Yu, B.-C. *ACS NANO* **2008**, *2*, 97. doi:10.1021/nn700294m.
(24) Butte, W. A.; Case, F. H. *J. Org. Chem.* **1961**, *26*, 4690. doi:10.1021/jo01069a513.
(25) Scott, J. D.; Puddephatt, R. J. *Organometallics* **1983**, *2*, 1643. doi:10.1021/om50005a028.
(26) Zhang, F.; Jennings, M. C.; Puddephatt, R. J. *Organometallics* **2004**, *23*, 1396. doi:10.1021/om030650m.
(27) Chatterjee, S.; Krause, J. A.; Madduma-Liyanage, K.; Connick, W. B. *Inorg. Chem.* **2012**, *51*, 4572. doi:10.1021/ic202462a.
(28) Nasser, N.; Borecki, A.; Boyle, P. D.; Puddephatt, R. J. *Inorg. Chem.* **2013**, *52*, 7051. doi:10.1021/ic400576m.
(29) Suwa, K.; Otsuki, J.; Goto, K. *J. Phys. Chem. A* **2010**, *114*, 884. doi:10.1021/jp909922y.
(30) Bortolus, P.; Monti, S. *J. Phys. Chem.* **1979**, *83*, 648. doi:10.1021/j100469a002.
(31) Zimmerman, G.; Chow, L. Y.; Paik, U. J. *J. Am. Chem. Soc.* **1958**, *80*, 3528. doi:10.1021/ja01547a010.
(32) Rau, H. In *Photochromism: Molecules and Systems*; Durr, H., Bouas-Laurent, H., Eds.; Elsevier: Amsterdam, 1990; pp. 165–192.
(33) Rau, H.; Luddeke, E. *J. Am. Chem. Soc.* **1982**, *104*, 1616. doi:10.1021/ja00370a028.
(34) Solomon, E. I.; Lever, A. B. P. *Inorganic Electronic Structure and Spectroscopy*; Wiley-Interscience: New York, 1999.
(35) Robinson, R.; Karikachery, A. R.; Sharp, P. R. *Dalton Trans.* **2012**, *41*, 2601. doi:10.1039/c2dt11594h.
(36) Connick, W. B.; Geiger, D.; Eisenberg, R. *Inorg. Chem.* **1999**, *38*, 3264. doi:10.1021/ic981387y.
(37) Chaudhury, N.; Puddephatt, R. J. *J. Organomet. Chem.* **1975**, *84*, 105. doi:10.1016/S0022-328X(00)88779-3.
(38) te Velde, G.; Bickelhaupt, F. M.; Baerends, E. J.; van Gisbergen, S.; Guerra, C. F.; Snijders, J. G.; Ziegler, T. *J. Comput. Chem.* **2001**, *22*, 931. doi:10.1002/jcc.1056.
(39) (a) Bruker-Nonius, *SAINT version 2012.12*, Bruker-Nonius: Madison, WI, 2012; (b) Bruker-Nonius, *SADABS version 2012.1*, Bruker-Nonius: Madison, WI, 2012.
(40) Burla, M. C.; Caliandro, R.; Camalli, M.; Carrozzini, B.; Cascarano, G. L.; Giacovazzo, C.; Mallamo, M.; Mazzone, A.; Polidori, G.; Spagna, R. *J. Appl. Cryst.* **2012**, *45*, 357. doi:10.1107/S0021889812001124.
(41) Sheldrick, G. M. *Acta Cryst. 2008*, *A64*, 112. doi:10.1107/S0108767307043930.